Characterization and Detection of Breast Cancer using Ultra Wideband Polarimetric Electromagnetic Transients

Characterization and Detection of Breast Cancer using Ultra Wideband Polarimetric Electromagnetic Transients

Hoi-Shun Lui
School of Information Technology and Electrical Engineering, The University of Queensland, Brisbane, Queensland 4072, Australia
Email: h.lui@uq.edu.au

Andreas Fhager, Jian Yang, Mikael Persson
Department of Signals and Systems
Chalmers University of Technology, Gothenburg, Sweden

Abstract—**Detection and recognition of metallic targets based on Ultra Wideband electromagnetic transients have been widely studied throughout the years. Due to the complexity of the scattering phenomena, such techniques have not been widely applied for dielectric targets. In this paper, the potential of detection and characterization of dielectric target is investigated. Instead of using single co-polarized linear responses, Ultra wideband polarimetric responses are considered. Numerical example of a breast cancer detection scenario will be used to demonstrate the feasibility of using wideband polarimetric data to characterize dielectric target.**

Keywords- microwave breast cancer detection, transient electromagnetic field, ultra wideband, dielectric targets

I. INTRODUCTION

In the last two decades, detection and imaging of tumor inside breast volumes using microwave technologies have been of significant interest. Currently, breast cancer detection and imaging are mainly performed using X-ray mammography and magnetic resonance imaging (MRI). Although mammography is currently used routinely in hospital, X-ray itself is ionizing which is cancerous to the subject. MRI is economically expensive which is not suitable for repeated screening. Compared to X-ray and MRI, microwave is non-ionizing and it is economically cheap. Under microwave illumination, the dielectric contrast between healthy glandular tissue and malignant tissue is higher as compared to the contrast under X-ray illumination [1]. With these motivations in mind, many research groups worldwide have been working on the problem.

Most groups have been focus on an imaging approach. In general, a cross sectional view of the breast volume is constructed based on measurements from various aspects of the breast volume. There are two ways to approach this problem, namely the radar-based approach [1] and the tomography approach [2]. The radar-based approach aims to identify the presence and location of the strong scatterer due to the huge contrast between the tumor and the glandular tissue. This involves focusing reflections from the breast volume, which is a coherent-sum process adapted from synthetic aperture radar (SAR) [1]. The resultant image is a spatial profile of intensities resulted from the coherent sum. On the other hand, the tomography approach aims to reproduce the dielectric profiles of the entire breast volume. This involves solving the inverse scattering problem [2] and the resultant images are the spatial distributions of the relative permittivity and conductivity.

Other than an imaging solution, a detection approach is considered in this paper. The breast volume is illuminated using a short electromagnetic pulse in time domain. These short pulses in time domain correspond to a wide bandwidth in frequency domain such that it falls under the Ultra Wideband (UWB) spectrum. The UWB pulses strike on the breast volume, de-polarize and scatter to all directions. The scattered signals contain the information about the geometrical and physical properties of the breast volume, which could be used as feature sets to classify the breast volume. Due to the huge dielectric contrast between the glandular tissue and malignant tumor, the existence of the tumor can potentially be detected based on these UWB transients.

Baum [3] proposed the Singularity Expansion Method (SEM) that describes the late-time period of the transient signature scattered from an object as a sum of damped exponentials. Such damped exponentials correspond to the Natural Resonant Frequencies (NRFs) of the object. Theoretically, these NRFs purely correspond to the physical and geometrical properties of the object and independent to the incident aspects and polarization [4], which allows it to be used as a feature set for classification. Automated target recognition (ATR) algorithms such as K-Pulse [5] and E-Pulse [6]-[8] are introduced. These pulses are essentially synthesized filter that annuls the resonance modes in the transient signatures when the right target is found.

Upon the proposition of SEM, most studies concern detection and recognition of metallic targets. Metallic targets have high-Q factors with small damping factor such that their NRFs can easily be extracted from the transients. Instead of metallic targets in free-space, recent attempts have also been made for monitoring and detecting subsurface metallic [9]-[11] and dielectric target [12] using these UWB transient signatures. In the context of microwave cancer detection, attempt has also been made to characterize tumors inside human tissue using NRF [13] and ATR using the E-Pulse [14].

To our knowledge, SEM and resonance-based target recognition have not been widely applied to dielectric objects. Theoretical study on dielectric and metallic sphere [15] shows that the NRFs of dielectric targets are relatively more damped, which could be difficult to extract from the transient response. Furthermore, electromagnetic wave penetrates into dielectric targets and resonant modes due to internal bouncing are established. These internal NRFs scatter in different polarization which could not be found in the co-polarized response. Overall, the scattering phenomena and resonance behavior of dielectric targets are more complicated than metallic targets. In addition, most studies in the context of resonance based target recognition are concerned with linear polarization excitation. Usually only the co-polarized component is considered.

To handle this problem, UWB transient responses under different polarization states are considered. Instead of using only one transient signature for NRF extraction, full polarimetric measurements are considered and the four polarimetric signatures will be used for NRF extraction simultaneously. In addition, the polarimetric features at the resonant frequencies will also be extracted. In cases where the targets have the same resonant frequency, the polarimetric features provide another degree of information for target characterization. To demonstrate the feasibility of using these features for target classification, numerical examples of some simple breast volumes with tumors will be presented. To our knowledge, the use of UWB polarimetric transients for automated target recognition has not been widely exploited in the literature.

II. Resonance-Based Target Recognition

Upon excitation of the target in free space using a short electromagnetic pulse, the late time of the target signature can be expressed as [3]-[8]

$$r(t) = \sum_{n=1}^{N} a_n e^{\sigma_n t} \cos(\omega_n t + \phi_n), \qquad t > T_l \qquad (1)$$

where a_n and ϕ_n are the aspect dependent amplitude and phase of the n^{th} mode and T_l is the onset of the late time period. It is assumed that only N modes are excited by the incident field. The NRFs are given by $s_n = \sigma_n \pm j\omega_n$, where σ_n and ω_n are the damping coefficients and resonant frequencies respectively. These complex resonances correspond purely to the physical properties of the target's geometry, dielectric properties and loss mechanisms and are theoretically aspect independent. Another attractive feature about these NRFs is that they are independent of the exciting wave's aspect and polarization. This is because these late-time resonances occur when the pulse has been propagated through the whole target, which is a global phenomenon. The NRFs are thus purely target dependant and therefore they can be used as a feature set for target identification. However, the amplitude and phase of the resonant mode (a_n and ϕ_n) varies as a function of aspect and polarization angle (consider linear polarization basis) [3]-[4] such that the amplitude of the resonant mode could be small such that it cannot be excited at certain polarization states.

III. Polarization in the Context of Coherent Scattering

Consider an orthogonal linear polarization basis with horizontal and vertical components, (H,V). In frequency domain, the relationship between the scattered electric field components $\vec{E}_s(H,V)$ and the incident electric field components $\vec{E}_i(H,V)$ from a target is given by [16]

$$\vec{E}_s(H,V) = \begin{bmatrix} S_{HH} & S_{HV} \\ S_{VH} & S_{VV} \end{bmatrix} \vec{E}_i(H,V) \qquad (2)$$

where $\vec{E}(H,V) = \begin{bmatrix} E_H e^{j\delta H} & E_V e^{j\delta V} \end{bmatrix}^T$, $E_H e^{j\delta H}$ and $E_V e^{j\delta V}$ are the horizontal and vertical electric field components. $[S(H,V)] = \begin{bmatrix} S_{HH} & S_{HV} \\ S_{VH} & S_{VV} \end{bmatrix}$ is the scattering matrix. The terms S_{HH}, S_{HV}, S_{VH} and S_{VV} correspond to the ratios between the incident and scattered electric field components. For instance, $S_{HV} = S_H^s / S_V^i$ corresponds to the ratio between scattered electric field in the horizontal polarization over the incident electric field in the vertical polarization. Note that the above description concerns the scattering phenomena at a particular frequency in the frequency domain.

IV. Polarization Description in Ultra Wideband

If we illuminate the target over a wideband of frequencies and apply an inverse Fourier transform to the wideband frequency domain data, the UWB scattering matrices in time domain can be written as

$$[S_{(H,V)}(t)] = \begin{bmatrix} S_{HH}(t) & S_{HV}(t) \\ S_{VH}(t) & S_{VV}(t) \end{bmatrix} \qquad (3)$$

Equivalently, the target can also be illuminated directly in time domain using short pulses in horizontal and vertical polarization and measures the co and cross scattered field.

According to (1), the late time period of each target signature can be written as a sum of damped exponentials. If we consider the n^{th} resonant mode, $s_n = \sigma_n \pm j\omega_n$, the corresponding complex Sinclair matrix $[A_n]$ can be given by the corresponding residues of each component [16]

$$[A_n]=\begin{bmatrix} a_{n,hh}e^{j\phi_{n,hh}} & a_{n,hv}e^{j\phi_{n,hv}} \\ a_{n,vh}e^{j\phi_{n,vh}} & a_{n,vv}e^{j\phi_{n,vv}} \end{bmatrix} \tag{4}$$

For monostatic configuration [7], the CPSs in terms of the antenna polarization ratios, P_i , where $i=1,2,3,4$ can be determined given the Sinclair matrix. The maximum backscattered power P_1 and P_2 at the resonant frequency can be given by

$$P_i=\frac{-\left|A_{n,xx}\right|^2+\left|A_{n,xy}\right|^2-\left|\gamma_i\right|^2}{A_{n,xx}A_{n,xy}+A_{n,xy}^{*}A_{n,yy}},$$

$$i=1,2\ ,\ \left|\gamma_1\right|^2,\ \left|\gamma_2\right|^2=\frac{B}{2}\pm\frac{\sqrt{B^2-4C}}{2} \tag{5}$$

where $B=\left|A_{n,xx}\right|^2+2\left|A_{n,xy}\right|^2+\left|A_{n,yy}\right|$ as well as $C=\left|A_{n,xx}A_{n,yy}\right|^2+\left|A_{n,xy}\right|^4-2\,\mathrm{Re}\left(A_{n,xx}A_{n,yy}^{*2}A_{n,yy}\right)$. The minimum backscattered power P_3 and P_4 are given by

$$P_3,P_4=\pm\frac{\left(\sqrt{A_{n,xy}^2-A_{n,xx}A_{n,yy}}\right)\mp A_{n,xy}}{A_{n,yy}} \tag{6}$$

The strokes parameters corresponding to the each polarization ratio P_i are

$$\frac{G_1}{G_0}=\frac{1-\left|P_i\right|^2}{1+\left|P_i\right|^2} \tag{7a}$$

$$\frac{G_2}{G_0}=\frac{2\,\mathrm{Re}(P_i)}{1+\left|P_i\right|^2} \tag{7b}$$

$$\frac{G_3}{G_0}=\frac{2\,\mathrm{Im}(P_i)}{1+\left|P_i\right|^2} \tag{7c}$$

The normalized strokes parameters corresponding to G_0 are given by

$$g=\begin{bmatrix} g_1 \\ g_2 \\ g_3 \end{bmatrix}=\frac{1}{G_0}\begin{bmatrix} G_1 \\ G_2 \\ G_3 \end{bmatrix} \tag{8}$$

The ellipticity ε and tilt angle τ of each polarization ratio as well as the characteristic angle β can be given by

$$\varepsilon=\frac{1}{2}\sin^{-1}\left(\frac{g_3}{\left(g_1^2+g_2^2+g_3^2\right)}\right), \tag{9a}$$

$$\tau=\frac{1}{2}\tan^{-1}\left(\frac{g_2}{g_1}\right), \tag{9b}$$

$$\tan^2\beta=\frac{\left|\gamma_2\right|}{\left|\gamma_1\right|}. \tag{9c}$$

The ellipticity and tilt angle describe the polarization ellipse of the corresponding polarization ratio P_i . The characteristic angle, also known as polarizability angle, is the target characteristic that causes the target to scatter an initially unpolarized wave as one with a great degree of polarization. For instance, the x and y components of an un-polarized wave are uncorrelated and have equal power densities. However, if an unpolarized wave incident on a target and backscatters the y but not the x component, the backscattered wave is polarized. A larger value of β indicates the target is less able to polarize wave than a target with a smaller value of β .

Here, we would like to investigate the scattering behavior of the target at NRF. As it will be seen shortly, the polarization ellipse of the scattered field and its polarizability at the corresponding resonant frequency provide further physical insight about the scattering process which could be used as an additional feature set for target characterization.

V. NUMERICAL EXAMPLES

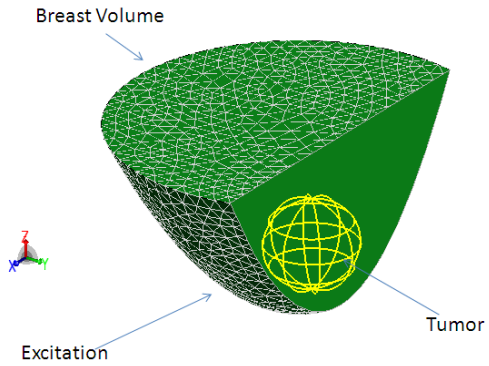

Fig. 1. The Breast volume under plane wave illumination

Numerical examples of a breast cancer detection setup using simple breast models are considered. The model is shown in Fig. 1. It is a hemisphere with radius of 60mm. The entire breast volume is illuminated from 23MHz to 3GHz with 128 samples in frequency domain. The incoming aspects of $\theta=105°$, $\phi=80°$ is considered (elevation angle of $\theta=0°$ corresponds to the positive z axis) and the scattered field is computed in the monostatic direction. The computation is done using commercial moment method solver FEKO in frequency domain [17]. In this example, three different breast volumes, i.e. (i) without tumor, (ii) with a 10mm tumor and

Frequency		Breast with no Tumor		Breast with 10mm tumor		Breast with 15mm tumor	
		(τ, ε)	β	(τ, ε)	β	(τ, ε)	β
1.98*GHz*	P_1	(0.013°, 0.013°)	5.02°	(-42.26°, 10.42°)	17.70°	(-60.74°, 5.59°)	30.28°
	P_2	(-89.98, -0.013°)		(47.73°, -10.42°)		(29.26°, -5.59°)	
	P_3	(-75.81°, -8.86°)		(39.78°, 18.06°)		(52.64°, 5.91°)	
	P_4	(75.84°, 8.84°)		(72.53°, -36.56°)		(-9.96°, -31.32°)	
2.56*GHz*	P_1	(0.08°,-0.0378°)	38.20°	(6.93°, 29.48°)	37.45°	(-0.42°, -9.19°)	18.81°
	P_2	(-89.91°, 0.0378°)		(-83.06°, -29.48°)		(89.57°, 9.19°)	
	P_3	(-53.06°,-32.29°)		(-13.95°, -16.13°)		(-58.88°, 6.81°)	
	P_4	(53.086°, 32.31°)		(78.79°, 8.93°)		(59.40°, 2.14°)	
2.75*GHz*	P_1	(-0.0013°, -0.031°)	2.69°	(76.89°, -33.07°)	42.46°	(15.15°, -32.64°)	16.87°
	P_2	(89.99°, 0.031°)		(-13.10°, 33.07°)		(-74.84°, 32.64°)	
	P_3	(84.31°, -10.87°)		(75.86°, 13.18°)		(30.34°,27.40°)	
	P_4	(-84.31°, 10.93°)		(-14.09°, -10.65)°		(-66.26°, 4.43°)	

Table 1. The tilt angle, ellipticity and characteristic angle of the dominant resonant modes of the breast volumes

(iii) with a 15 mm tumor, will be considered. For the latter two cases, a dielectric sphere with the relative permittivity of $\varepsilon_r = 50$ and a radius of 10mm and 15mm respectively, centres at the position of ($15mm$, $15mm$, $30mm$), is added in the FEKO environment to mimic the tumor.

In each case, the co- and cross- polarized target signatures, i.e. the four polarimetric signatures in (3), are obtained. The frequency samples are then windowed via a Gaussian window with the time profile starting at 10ns. The late time commences on 12ns and samples from 12ns onwards are imported to the modified matrix pencil method (MPM) [18]-[19] for resonant extractions. Compared to the original MPM [18], the modified MPM [19] is able to handle all 4 target signatures at the same time such that only one set of NRFs and 4 sets of residues will be resulted.

The results are tabulated in Table 1. The first three dominated resonant frequencies at 1.98GHz, 2.56GHz and 2.75GHz are founded from the NRF extraction and their corresponding polarization features are tabulated in Table 1. When there is no tumor, the polarization ratios that give the maximum backscattered power (P_1 and P_2) are linearly polarized (with $\varepsilon \approx 0°$) and indicate that the target is symmetric ($\tau \approx 0°$). When there is a tumor, they become elliptically polarized and the ellipticity τ increases as the resonant frequency increases. The tilt angle and ellipiticity of P_3 and P_4 have the same magnitudes but with different signs for the case when there is no tumor, which further confirms that the target is symmetric. Comparing the characteristic angles at the same resonant frequency for the three cases, they are quite different from each other which distinguish their capabilities to de-polarize the incident wave at those frequencies.

Apparently, the polarimetric features of the scattered field at the resonant frequencies are very different comparing the cases with and without the tumor. The results here demonstrate another degree of information about the scattering behavior at resonant frequencies. Such information does not only provide further physical insight about the scattering behavior at the resonant frequencies, they can also be used as an additional feature set for target classification. For ATR purpose, for example, the four polarization ratios can be plotted on a Poincare sphere and forms an interesting pattern known as the Huynen fork [16].

VI. CONCLUSIONS

The potential of using UWB polarimetric responses for characterization of dielectric targets is considered. In particular, dielectric hemispheres embedded with a small sphere are used to mimic the scenarios of breast cancer detection. The characteristic polarization states at the resonant frequencies are evaluated and found that the scattering behavior at the resonant frequencies are significantly different which indicates that these polarimetric features can be used as an additional feature set for target classification. In particular, in cases where the library of targets has similar resonant frequencies, the polaritmetric features provide additional information to distinguish the targets.

The results presented in this work demonstrate the potential of incorporating different features extracted from UWB polarimetric target signatures. Future work should focus on novel target classification and recognition procedures as well as its capabilities for breast cancer detection using electrically and geometrically realistic breast models [20].

REFERENCES

[1] E. C. Fear, S. C. Hagness, P. M Meaney, M. Okoniewski and M. A. Stuchly, "Enhancing Breast Tumor Detection with Near-Field Imaging", *IEEE Microwave Magazine*, Vol. 48, pp. 48-56, Mar. 2002

[2] A. Fhager and M. Persson, "Using a priori Data to Improve the Reconstruction of Small Objects in Microwave Tomography", *IEEE Trans. Microwave Theory and Techniques* , Vol. 55, No. 11, pp. 2454-2462, Nov. 2007

[3] C. E. Baum, E. J. Rothwell, K. M. Chen and D. P. Nyquist, "The Singularity Expansion Method and Its Application to Target Identification", *Proc. IEEE*, Vol. 79, No.10, pp 1481-1491, Oct. 1991.

[4] N. Shuley and D. Longstaff, "Role of polarisation in automatic target recognition using resonance descriptions", *Electronics Letters*, Vol. 40, No. 4, pp. 268-270, 2004.

[5] E. N. Kennaugh, "The K-Pulse Concept", *IEEE Trans. Antennas Propag*., Vol. 29, No. 2, pp 327-331, Mar., 1981.

[6] E. J. Rothwell, D. P. Nyquist, K. M. Chen, and B. Drachman, "Radar target discrimination using the extinction-pulse tech-nique," *IEEE Trans Antennas Propag.*, vol. AP-33, pp. 929-937, Sept. 1985.

[7] H. S. Lui, N. V. Z. Shuley, "Radar Target Identification using a "Banded" E-Pulse technique", *IEEE Trans. Antennas Propag*., Vol. 54, No. 12, pp 3874-3881, Dec., 2006.

[8] H. S. Lui, N. V. Z. Shuley, "Sampling Procedures in Resonance Based Radar Target Identification*", IEEE Trans. Antennas Propag*., Vol. 56, No. 5, pp. 1487-1491, May 2008

[9] H. S. Lui, N. V. Z. Shuley, "Detection of Depth Changes of a Metallic Target Buried inside a Lossy Halfspace Using the E-Pulse Technique", *IEEE Trans. Electromagnetic Compatibility*, Vol. 49, No. 4, pp. 868-875, November 2007

[10] H. S. Lui, F. Aldhubaib, N. V. Z. Shuley, H. T. Hui, "Subsurface Target Recognition based on Transient Electromagnetic Scattering", *IEEE Trans. Antennas Propag.*, Vol. 57, No. 10, pp. 3398-3401, Oct. 2009

[11] H. S. Lui, N. V. Z. Shuley, A. D. Rakic, "A Novel, Fast, Approximate Target Detection Technique for Metallic Target below a Frequency Dependent Lossy Halfspace", *IEEE Trans. Antennas Propag.*, Vol. 58, No. 5, pp. 1699-1710, May 2010

[12] S. K. Padhi, H. S. A. Lui, N. V. Shuley, "Identification of an Unknown Dielectric Target in a Half-Space Using the E-Pulse Technique*", Radio Science*, Vol 43, No 5, 10.1029/2007RS003731, Oct. 2008

[13] Y. Huo, R. Bansal and Q. Zhu, "Modeling of Noninvasive Microwave Characterization of Breast Tumors", *IEEE Trans. Biomedical Engineering*. Vol. 51, No. 07, pp 1089-1094, Jul. 2004.

[14] H. S. Lui, B. K. Li, N. Shuley, S. Crozier "Preliminary Investigation of Breast Tumor Detection Using the E-Pulse Technique", *Proceedings of IEEE Antenna and Propagation Society International Symposium USNC/URSI National Radio Science Meeting*, pp. 283-286, 9 – 14 July, 2006, Albuquerque, New Mexico, USA

[15] C. C. Chen, "Electromagnetic resonances of Immersed Dielectric Spheres", *IEEE Trans. Antennas Propag.*, Vol. 46, No.7, pp 1074-1083, July, 1998.

[16] H. Mott, *Remote Sensing with Polarimetric Radar*, John Wiley & Sons, 2007.

[17] FEKO EM Software & Systems S.A., (Pty) Ltd, 32 Techno Lane, Technopark, Stellenbosch, 7600, South Africa

[18] T. K. Sarkar and O. Pereira, "Using the Matrix Pencil Method To Estimate the Parameters of a sum of Complex Exponentials", *IEEE Antennas Propag. Magazine*, Vol. 37, No. 1, pp. 48-55, Feb. 1995.

[19] T. K. Sarkar, S. Park, J. Koh, S.M. Rao, "Application of the Matrix Pencil Method for Estimating the SEM (Singularity Expansion Method) Poles of Source-Free transient Responses from Multiple look Directions", *IEEE Trans. Antennas Propag.,* Vol. 48, No.4, pp. 612-618, Apr., 2000.

[20] H. S. Lui, M. Widmark, G. Starck, Y. Li, M. Persson, "Development of patient-specific breast electromagnetic model bsaed on clinical magnetic resonance images," *IEEE International Symposium of Antennas and Propagation Society (AP-S)*, Toronto, Canada, pp. 1-4, 2010